Binding of a non-ionic pyrenylisoxazolidine derivative to double-stranded polynucleotides: spectroscopic and molecular modelling studies†

Antonio Rescifina,*[a] Ugo Chiacchio,[a] Anna Piperno[b] and Salvatore Sortino*[a]

Received (in Montpellier, France) 5th December 2005, Accepted 31st January 2006
First published as an Advance Article on the web 22nd February 2006
DOI: 10.1039/b517150d

The binding of [(3*RS*,5*SR*)-2-methyl-3-pyren-1-ylisoxazolidin-5-yl]methanol (MPIM), a non-ionic pyrene derivative with potential anticancer activity, to calf-thymus DNA (ct-DNA) and the synthetic double-strand polynucleotides poly-d(AT)$_2$ and poly-d(GC)$_2$ was investigated at neutral pH through the combination of UV-Vis absorption and emission spectroscopy, fluorescence quenching experiments and molecular modelling studies. Hypochromic effects accompanied by the formation of tight isosbestic points were observed upon binding of MPIM to polynucleotides. The related binding constants, evaluated by the half-reciprocal plots of the absorbance data, were 6.8×10^3 M^{-1}, 6.0×10^3 M^{-1} and 1.5×10^3 M^{-1} for ct-DNA, poly-d(AT)$_2$ and poly-d(GC)$_2$, respectively. The fluorescence emission intensity of MPIM was slightly quenched by ct-DNA, basically unaffected by poly-d(AT)$_2$ and efficiently suppressed by poly-d(GC)$_2$. The overall results support an intercalative binding mode of the pyrene derivative in the case of ct-DNA and poly-d(AT)$_2$, whereas a shallow intercalation seems to be involved with poly-d(GC)$_2$. Docking studies agree with the experimentally observed complex stability order and reveal a common binding mode implying that the chromophore intercalates between the staked base pairs and the isoxazolidine ring lying along the major groove. In any case a stabilizing hydrogen bond is formed between the hydroxyl group of the MPIM methanol moiety and the oxygen of a phosphate group. The preferential binding selectivity of MPIM for intercalation in AT-rich regions is probably attributable to steric hindrance between the *N*-methyl group of MPIM and the 4-amino one of the cytosine in the GC sites.

Introduction

Intercalation with nucleic acids is one of the most important cytostatic mechanisms of action of coplanar annelated polycyclic compounds.[1] A variety of natural and synthetic agents exhibiting this binding mode show, in fact, excellent anticancer activity. Of these, anthracyclines,[2] acridines[3] and ellipticines[4] constitute some of the most significant examples. However, less attention has been paid to the binding of simple polycyclic hydrocarbons bearing either the anthracene or pyrene ring.[5] These compounds generally bind to DNA through non-specific intercalations between the base pairs.[6] Nevertheless, in the case of some cationic derivatives, evidence indicating a preference for alternate AT sequences over GC sequences has been reported.[7–10] Such base selectivity has been attributed to the variation of the local structure induced by the electrostatic interaction with DNA.

In a recent paper, some of us have reported the synthesis and the biological activity of novel non-ionic potential anticancer agents characterized by the presence of polycyclic aromatic nuclei, functionalized with an isoxazolidine ring.[11] The reasons at the basis of this design were that (i) the fused polyaromatic system should allow effective DNA intercalation and (ii) the isoxazolidine sub-unit could promote a certain degree of base selectivity assuring, at the same time, a desirable regioselective functionalization of the polycyclic core through easy synthetic manipulations. Among the investigated compounds [(3*RS*,5*SR*)-2-methyl-3-pyren-1-ylisoxazolidin-5-yl]-methanol (MPIM) exhibited promising cytotoxic and apoptotic properties. In light of this, we considered it of importance to shed light on the interaction of MPIM with DNA. This can be helpful not only for a better understanding of the biological function of the drug at the molecular level but also in the perspective of new drug design. To this end, in this paper we investigate the binding of MPIM to calf-thymus DNA (ct-DNA) and two synthetic double-strand polynucleotides, poly-d(AT)$_2$ and poly-d(GC)$_2$, by combining UV-Vis absorption and emission spectroscopic techniques, fluorescence quenching experiments and molecular modelling studies.

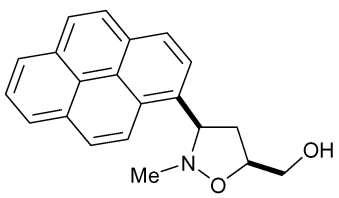

MPIM

[a] *Dipartimento di Scienze Chimiche, Università di Catania, Viale Andrea Doria 8, I-95125 Catania, Italy. E-mail: ssortino@unict.it*
[b] *Dipartimento Farmaco-Chimico, Università di Messina, Via SS. Annunziata, I-98168 Messina, Italy*

† Dedicated to Dr Sandra Monti, excellent scientist and good friend, on the occasion of her 60th birthday (S. S.).

Experimental

Sonicated ct-DNA (phenol extracted, lyophilized, average size 2000 bases, range 200–6000 bases) was obtained from Pharmacia (Milan). The synthetic polynucleotides poly-d(AT)$_2$ and poly-d(GC)$_2$, and NaI were purchased from Sigma (Milan) and used without further purification. MPIM was synthesized as recently reported by some of us[11] through 1,3 dipolar cycloaddition reaction methodology.[12] Water was purified through a Millipore Milli-Q system. All experiments were conducted in 10^{-2} M phosphate buffer at pH 7.4, containing 0.1 M NaCl. The pH of the solution was measured with a glass electrode. The concentrations of polynucleotides, in base pairs, were determined by absorption spectroscopy, using the following molar extinction coefficients: ct-DNA, 6600 M^{-1} cm^{-1} at 260 nm; poly-d(AT)$_2$, 6600 M^{-1} cm^{-1} at 260 nm; poly-d(GC)$_2$, 8400 M^{-1} cm^{-1} at 254 nm.[13] Absorption and emission spectra were recorded with a Beckman 650 DU spectrophotometer and a Spex Fluorolog-2 (mod. F-111) spectrofluorimeter, respectively. All the spectra were corrected for the dilution resulting from addition of polynucleotide solutions to the solution of MPIM.

Calculations were carried out with the Amber96 force field, that is one of the most accurate force fields widely used for proteins and DNA,[14] as implemented in the HyperChem 7.5 program package.[15] Poly-d(AT)$_2$ and poly-d(GC)$_2$ were simulated as hexamer fragments of (dA-dT)$_2$ and (dG-dC)$_2$, respectively, whereas for the ct-DNA was chosen the palindromic decamer fragment d(CGCAATTGCG)$_2$. The hexamer fragments were constructed with the nucleic acids tool in the B-DNA conformation; the decamer fragment was retrieved from Brookhaven Protein Database (ID: 252D) and the crystallographic water molecules were deleted. All fragments were 3′- and 5′-endcapped with a phosphate group and the system configured as a fully anionic oligonucleotide with monovalent sodium cations placed initially at positions bifurcating the O–P–O angle at 4.0 Å from the phosphorus atom. Subsequently, the geometry was fully minimized with a convergence criterion of 0.01 kcal mol^{-1} per Å, by assigning a distance-dependent dielectric of 1.0, 1–4 scale factors of 0.833 for the electrostatic part and of 0.5 for the van der Waals part, and the non-bonded cutoff set to off.

The simulations of the MPIM bound to poly-d(AT)$_2$, poly-d(GC)$_2$ and ct-DNA were carried out using docking methodology.[16] Firstly, the MPIM was selected to insert into the middle base-step of each fragment either from the minor or the major groove. While the MPIM atom positions were fixed, the remaining oligonucleotide was minimized in order to suitably accommodate the MPIM molecule. Subsequently the whole system was minimized with a convergence criterion of 0.05 kcal mol^{-1} per Å, without any restraints.

Molecular docking calculations were performed using the software GRAMM.[17] In a typical calculation the MPIM molecule was deleted from the previously obtained complexes, so making a free pocket in the d(AT)$_2$, d(GC)$_2$ and ct-DNA fragments. Then molecular docking was allowed to take place between the MPIM ligand and the arranged target fragment, employing high-resolution parameters, and the structures obtained from the ten best scores were ulteriorly refined with a convergence criterion of 0.01 kcal mol^{-1} per Å.

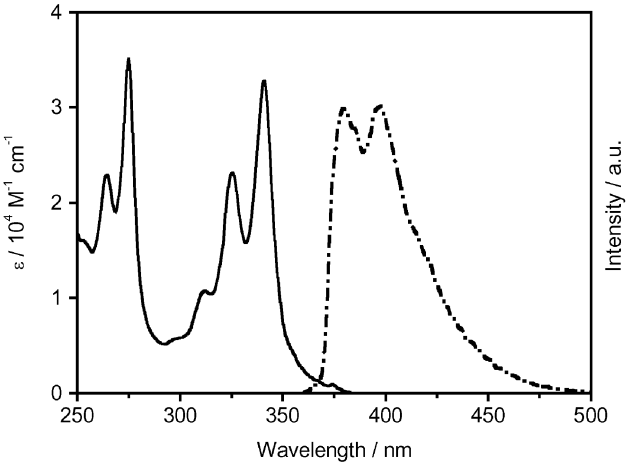

Fig. 1 Absorption (—) and fluorescence (---) spectra of MPIM in 10^{-2} M phosphate buffer at pH 7.4.

Results

The presence of the polar isoxazolidine substituent increases the solubility of MPIM in aqueous solution when compared to pyrene itself. Fig. 1 shows the absorption and fluorescence spectra of MPIM in neutral aqueous buffer solution. The spectral features observed are fairly similar to those of pyrene in water[18] and suggest that the presence of the isoxazolidine substituent does not appreciably affect the electronic properties of the pyrene unit. Therefore, analogously to pyrene, the absorption and emission properties of MPIM are expected to be sensitive to the local microenvironment and, as a consequence, represent a suitable spectroscopic tool by which to inspect the interaction with nucleic acids.[19]

Fig. 2(A)–(C) report the absorption spectral changes observed upon addition of either ct-DNA or synthetic polynucleotides to solutions of MPIM in 10^{-2} M phosphate buffer at pH 7.4. In the case of ct-DNA and poly-d(AT)$_2$ the absorption bands at 326 and 342 nm undergo strong hypochromism (>60%) and a new absorption appears at 355 nm. In both cases very tight isosbestic points at 347 nm are also observed, suggesting homogeneity of the binding process. On the other hand, in the case of poly-d(GC)$_2$ the hypochromic effect is much smaller and the absorption at 355 nm is barely perceptible. These results provide a first, clear indication for the formation of ground-state complexes of MPIM with the three biopolymers.

In order to obtain the binding constants, K_b, related to association complexes we used the half-reciprocal plot of the absorption titration data, according to eqn (1):[20]

$$[P]_{bp}/(\varepsilon_A - \varepsilon_F) = [P]_{bp}/(\varepsilon_B - \varepsilon_F) + 1/K_b(\varepsilon_B - \varepsilon_F) \qquad (1)$$

Here $[P]_{bp}$ is the concentration of the polynucleotide in base pairs, ε_A, ε_F and ε_B correspond to A_{obs}/[MPIM], the extinction coefficient for the free MPIM and the extinction coefficient for the totally bound form of MPIM, respectively.[1b,20] By the ratio of the slope to the intercept of the linear plots reported in

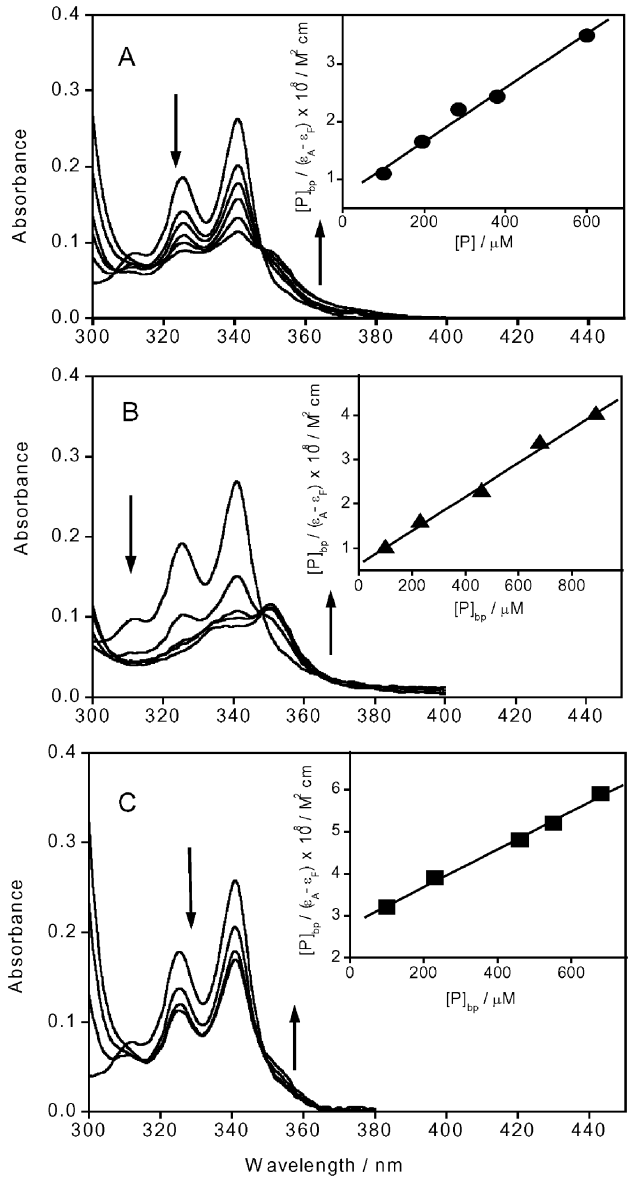

Fig. 2 Absorption spectral changes of MPIM (7.8×10^{-6} M) in 10^{-2} M phosphate buffer, at pH 7.4, in the presence of increasing amounts of (A) ct-DNA, (B) poly-d(AT)$_2$ and (C) poly-d(GC)$_2$, in the range $0-0.9 \times 10^{-3}$ M (some spectra are omitted for the sake of clarity). Cell path: 1 cm. The insets show the half-reciprocal plots of the binding of MPIM with the biopolymers determined at 340 nm.

the insets of Fig. 2, K_b values of 6.8×10^3 M^{-1}, 6.0×10^3 M^{-1} and 1.5×10^3 M^{-1} were found for ct-DNA, poly-d(AT)$_2$ and poly-d(GC)$_2$, respectively. These data point to some preference of MPIM for the alternating d(AT) sequences.

The interaction of MPIM with the biopolymers is also confirmed by fluorescence measurements. Fig. 3 illustrates the emission spectra of MPIM in the presence of increasing amounts of ct-DNA and recorded by exciting all the samples at the isosbestic point (347 nm). This wavelength was chosen in order to circumvent the trivial changes in the fluorescence intensity associated with variation in absorbance.

Addition of ct-DNA moderately quenches the fluorescence of MPIM and also induces a slight change in the ratio between

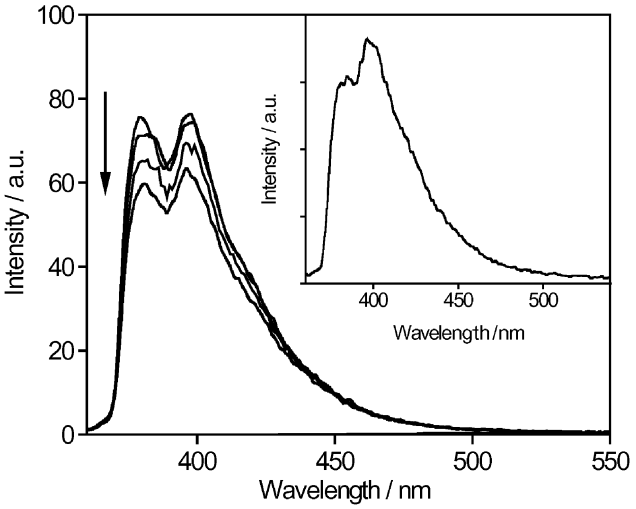

Fig. 3 Fluorescence emission spectra of MPIM (7.8×10^{-6} M) in 10^{-2} M phosphate buffer, at pH 7.4, with increasing amounts of ct-DNA in the range $0-0.9 \times 10^{-3}$ M and recorded at $\lambda_{exc} = 347$ nm. The inset shows the fluorescence emission spectrum of MPIM recorded at $\lambda_{exc} = 355$ nm, in the presence of the highest concentration of ct-DNA.

the vibronic bands. This latter effect is better perceptible when the sample is excited at 355 nm (inset Fig. 3), where the absorption of the bound form of MPIM dominates over that of the free one [see Fig. 2(A)].

The fluorescence response of MPIM to the addition of poly-d(AT)$_2$ at $\lambda_{exc} = 355$ nm is displayed in Fig. 4. It can be noted that the ratio of the two emission bands dramatically changes whereas the fluorescence intensity slightly increases. In particular, the emission of the almost totally bound species is characterized by a single fluorescence maximum at 400 nm. This is further supported by the excitation spectrum recorded

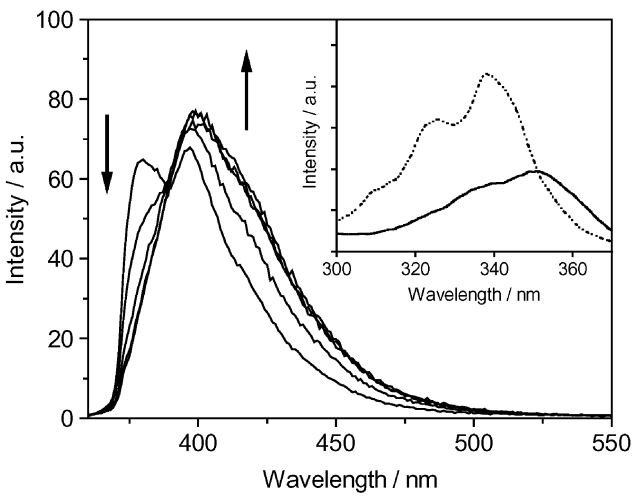

Fig. 4 Fluorescence emission spectra of MPIM (7.8×10^{-6} M) in 10^{-2} M phosphate buffer, at pH 7.4, in the presence of increasing amounts of poly-d(AT)$_2$ in the range $0-0.9 \times 10^{-3}$ M and recorded at $\lambda_{exc} = 355$ nm (all the spectra are corrected for the same amount of absorbed photons). The inset shows the fluorescence excitation spectrum of MPIM recorded in the presence of the highest concentration of poly-d(AT)$_2$ (—) and, for comparison, in its absence (···) at $\lambda_{em} = 400$ nm.

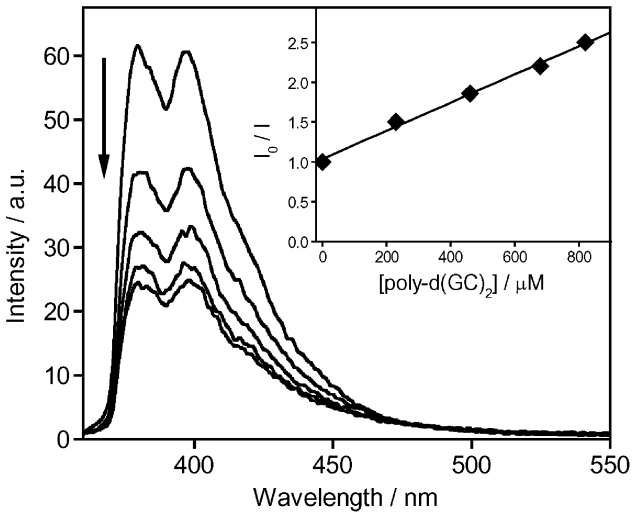

Fig. 5 Fluorescence emission spectra of MPIM (7.8×10^{-6} M) in 10^{-2} M phosphate buffer, at pH 7.4, in the presence of increasing amounts of poly-d(GC)$_2$ in the range 0–0.9×10^{-3} M and recorded at $\lambda_{exc} = 355$ nm (all the spectra are corrected for the same amount of absorbed photons). The inset shows the Stern–Volmer plot related to the fluorescence quenching of MPIM by poly-d(GC)$_2$.

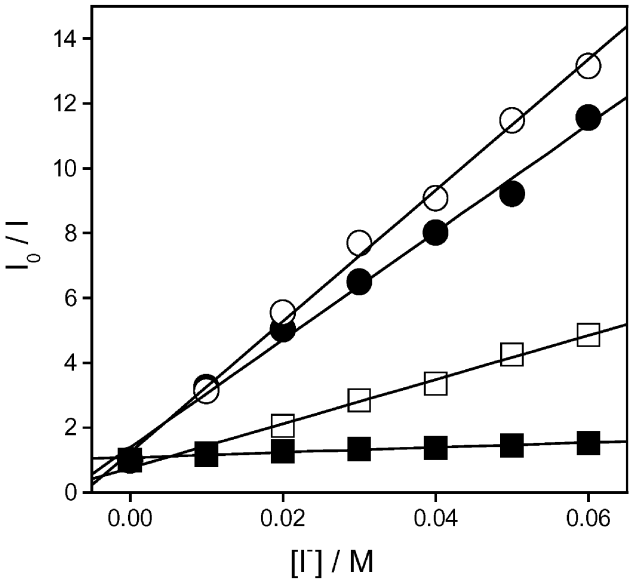

Fig. 6 Stern–Volmer plots for MPIM (7.8×10^{-6} M) fluorescence quenching by I^- in 10^{-2} M phosphate buffer, pH 7.4 in the absence (○) and in the presence of (□) ct-DNA, (■) poly-d(AT)$_2$ and (●) poly-d(GC)$_2$. The concentration of the polynucleotides was 1 mM.

at $\lambda_{em} = 400$ nm at high polynucleotide/fluorophore ratio. As shown in the inset of Fig. 4, the excitation spectrum recorded under the above experimental conditions reflects quite well the absorption spectrum observed at the same polynucleotide/fluorophore ratio [see Fig. 2(B) for comparison].

Addition of increasing amounts of poly-d(GC)$_2$ to a solution of MPIM, does not affect the fluorescence spectral shape, but, in contrast to the previous cases, efficiently quenches the emission intensity (Fig. 5).

By taking into account that the concentration range of the polynucleotide used is too low for a dynamic quenching mechanism of the excited singlet state of MPIM to be effective, it appears evident that a static quenching mechanism comes into play. In this regard, when the existence of different types of MPIM–poly-d(GC)$_2$ complexes is considered, with association constants K_i and relative fluorescence quantum yields Φ_i, the ratio of fluorescence intensities in the absence (I_0) and in the presence (I) of poly-d(GC)$_2$ is given by the following equation:[21]

$$I_0/I = (1 + \Sigma K_i[\text{poly-d(GC)}_2])/(1 + \Sigma \Phi_i K_i[\text{poly-d(GC)}_2]) \quad (2)$$

Since our results show that the fluorescence of the molecules bound to DNA is much lower than that of the free chromophores, we can assume that the MPIM–poly-d(GC)$_2$ complexes are basically non-fluorescent.[21] As a consequence, eqn (2) reduces to the familiar Stern–Volmer equation:

$$I_0/I = 1 + K_b[\text{poly-d(GC)}_2] \quad (3)$$

where $K_b = K_{SV} = \Sigma K_i$ is related to the different types of complexes not distinguishable by fluorescence.[22] The value of K_b obtained from the linear plots reported in the inset of Fig. 5 is 1.6×10^3 M^{-1}. This result is in excellent agreement with that obtained by absorption data and lends credibility to the model proposed.

More insights into the binding affinity of MPIM to nucleic acids are gained by fluorescence quenching experiments carried out in the presence of iodide. This anion quenches the fluorescence at near diffusion-controlled rate and is not easily accessible to the DNA interior due to the electrostatic field surrounding the helix.[23] Therefore, comparative experiments performed in the absence and in the presence of polynucleotides provide a sensitive method by which to establish if the fluorophore is deeply incorporated into the DNA helix.[23] The results of the quenching experiments were plotted according to Stern–Volmer eqn (4), where I_0 and I are the fluorescence intensities in the absence and in the presence of iodide, respectively, K_{SV} is the Stern–Volmer quenching constant and [I^-] is the molar concentration of iodide:

$$I_0/I = 1 + K_{SV}[I^-] \quad (4)$$

K_{SV} values were obtained from the slopes of the linear plots reported in Fig. 6. As expected, the K_{SV} value is the highest for the free fluorophore, 205 M^{-1}, and decreases in the presence of the different polynucleotides, being 160, 76 and 7 M^{-1} for poly-d(GC)$_2$, ct-DNA and poly-d(AT)$_2$, respectively.

To further support the above presented results as well as to gain more insight both into the modality of MPIM insertion, *i.e.* from the minor or the major groove, and the factors stabilizing the MPIM–DNA complex, we performed a docking study at the molecular mechanics level of calculations utilising the Amber96 force field (see experimental section). The binding energies (E_B) of the intercalation complexes (Table 1) were calculated by subtraction from the quantity of the complex ($E_{complex}$) the sum of the quantities of MPIM (E_{MPIM}) and either hexamer or decamer fragment ($E_{fragment}$), eqn (5):

$$E_B = E_{complex} - (E_{MPIM} + E_{fragment}) \quad (5)$$

Table 1 Calculated binding energies for MPIM complex with AT, GC and B-DNA fragments

Complex	E_b major groove	E_b minor groove
AT hexamer–MPIM[a]	−112.94[b]	−44.33
GC hexamer–MPIM[a]	−87.65	−57.25
B-DNA decamer–MPIM[a]	−125.26	−82.25
B-DNA decamer–MPIM[c]	−35.73	−42.80

[a] Complex achieved by MPIM intercalation between base pairs. [b] All energies are expressed in kcal mol^{-1}. [c] Complex achieved by MPIM binding along the groove.

It is important to note that the calculated interaction energies used to obtain a MPIM binding affinity ranking of the target sequences are not directly comparable to the experimental binding affinities. Contributions originating from (i) restrictions of the translational and orientational degrees of freedom and (ii) reduction of oligonucleotide and ligand vibrational degrees of freedom, upon binding, have not been considered. It should be stressed that although these terms make a significant, unfavourable, contribution to the absolute ligand –oligonucleotide binding free energy, they have only a small influence on the ranking mentioned above. Moreover, the solvation binding energy was overlooked inasmuch as the solvent accessible surface areas for the hexamer complexes have almost the same value; the same holds for all the decamer complexes, even those involved in groove binding. Then, although the so calculated binding energies have not a quantitative meaning, they indicate, at a qualitative level, that in all the cases the approach for the intercalative binding of MPIM takes place from the major groove side. Furthermore, these binding energies accord with the experimental order of the complex stability obtained by absorption data. In order to exclude the possibility of a binding mode along the major or minor groove, we have also calculated these binding energies starting from the twenty best score results obtained docking the MPIM with the B-DNA decamer as it is, *i.e.* without the pocket. The obtained results (see Table 1) are several kcal mol^{-1} above those obtained for intercalation, with a slight preference for the minor groove.

The greater stability of complexes arising from the major groove approach is due to the best π–π interactions between the pyrene chromophore and the stacked base pairs inasmuch as the aromatic planar moiety inserts with its longitudinal axis in a quasi-parallel mode with respect to the axis joining the base pairs >Fig. 7(A) and 7(B)]. On the other hand, in the approach from the minor groove, the longitudinal axis of the chromophore is quasi-orthogonal with respect to the same axis joining the base pairs and the pyrene ring protrudes to the major groove side, decreasing the π–π interactions [Fig. 7(C) and 7(D)].

In any cases, all intercalation complexes are additionally stabilized by hydrogen bonds. In particular, for the complex of MPIM with the B-DNA decamer fragment a hydrogen bond is formed between the hydroxyl group of the MPIM methanol moiety and the oxygen of a phosphate group, in the case of insertion from the major groove (Fig. 8, top). As far as the insertion from the minor groove is concerned a hydrogen bond between the same hydroxyl group of MPIM and the oxygen at the 2 position of the thymine is observed (Fig. 8, bottom).

The preference for intercalation of MPIM into the AT sites seems due to steric hindrance between the *N*-methyl group of MPIM and the 4-amino one of the cytosine in the GC sites that constrain the chromophore to deviate from the preferential approach in which its longitudinal axis is almost parallel to that of the base pairs.

Discussion

The above results allow some insight into the binding characteristics of MPIM with double-stranded polynucleotides. Generally, one pertinent question arising whenever the binding nature of drugs to DNA is investigated, is whether the ligand is intercalated or not in the DNA helix. Some of the above results reflect common features with typical intercalators. In particular, the strong hypochromism, the clear isosbestic

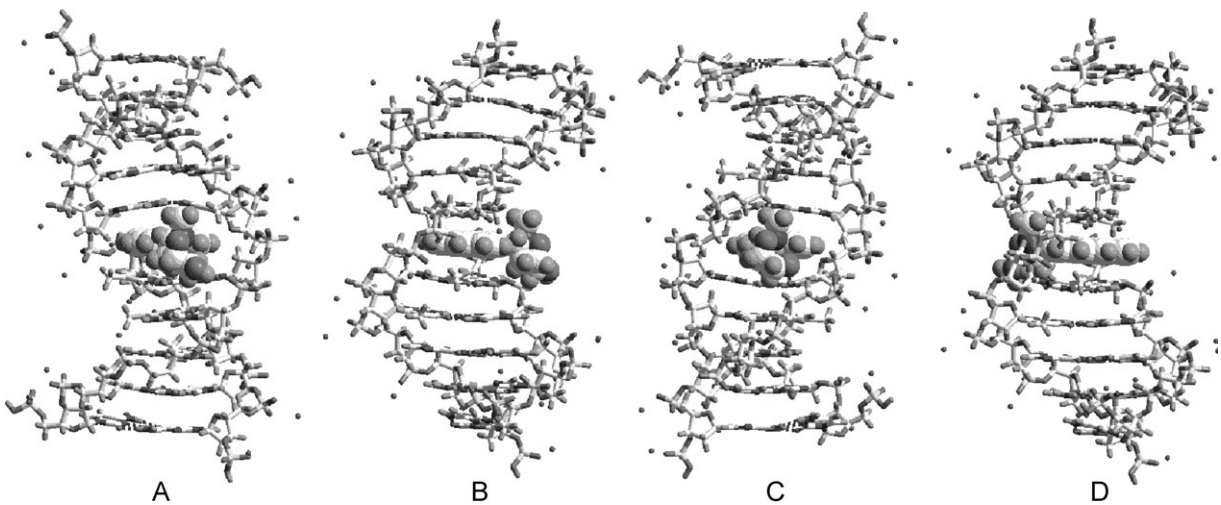

Fig. 7 Plots representing the intercalated MPIM as a CPK model and the DNA backbone as tube. (A) Front view and (B) side view with the isoxazolidine moiety placed in the major groove. (C) Front view and (D) side view with the isoxazolidine moiety placed in the minor groove.

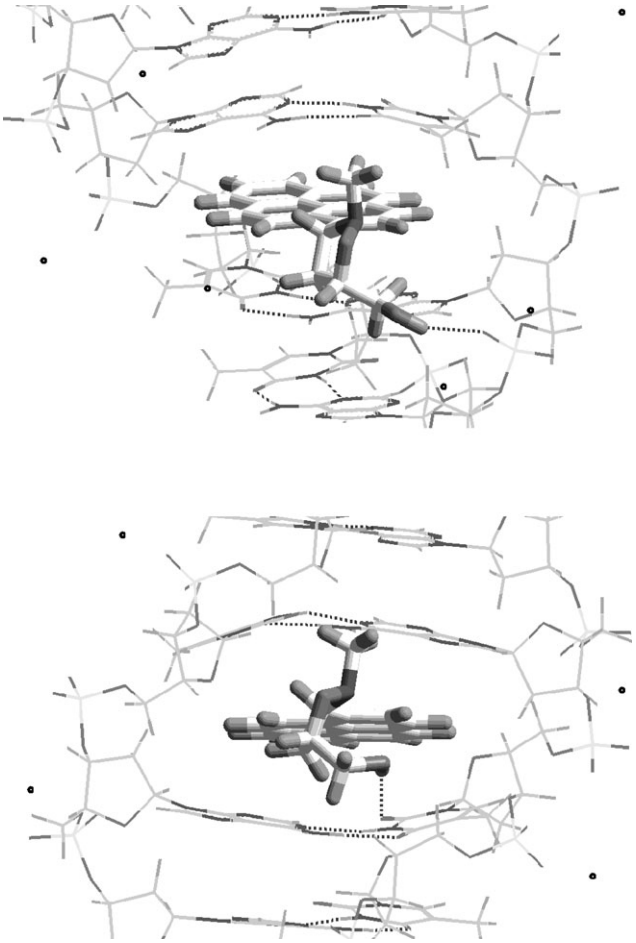

Fig. 8 Plot representing the intercalated MPIM as a tube model and the DNA backbone as wireframe. Front view with the isoxazolidine moiety placed (top) in the major and (bottom) in the minor groove.

points and the appearance of the new absorption at 355 nm observed in the presence of ct-DNA and poly-d(AT)$_2$ are very similar to those noted for other pyrene derivatives[10,24–26] and are accepted as a confirmation of proximity of the polycyclic hydrocarbon to the DNA core.[27] Hypochromism is due to a strong interaction between the electronic states of the intercalated chromophore and those of the DNA bases and the strength of this interaction is expected to decrease as the cube of the distance of separation between the chromophore and the DNA bases.[28] Thus, the effects we observed are consistent with the localization of the pyrene chromophore close to the DNA interior, providing a clear indication for the intercalation of MPIM into the DNA base stack. The same conclusions originate from molecular docking studies indicating that the value of the binding energy, in the case of the MPIM and B-DNA complex, is much more negative for the intercalation mode than for an interaction along the DNA grooves (see Table 1).

In general, the narrow range of hypochromism values observed with different synthetic polynucleotides indicates non-specificity for the DNA sequences.[10] However, this is not the case. In fact, the smaller hypochromic effect observed with poly-d(GC)$_2$ [see Fig. 2(C)] together with the barely appreciable absorption at 355 nm emphasize a more shallow intercalation of MPIM into this polynucleotide. The quantitative aspects of the interaction of the pyrene derivative with the biopolymers are strictly in line with the lower preference of MPIM for the alternating d(GC) base pairs. The binding constant with this polynucleotide is in fact *ca.* 4-fold smaller than that with poly-d(AT)$_2$.

The more favoured intercalative binding of MPIM to the AT sites is further supported by the fluorescence results. The emission of the complex of MPIM with poly-d(AT)$_2$ is comparable to that of the free fluorophore in terms of intensity but differs in the spectral shape (see Fig. 4). In this regard, it is worth recalling that pyrene is a very polarity-sensitive probe and its fluorescence is extensively employed to characterize microheterogeneous systems, since the ratio between the fluorescence bands is indicative of the microenvironment polarity.[29,30] Accordingly, the dramatic change in the ratio of the two emission bands observed upon binding of MPIM to poly-d(AT)$_2$ (Fig. 4) represents strong evidence for the confinement of the pyrene nucleus within a microenvironment of reduced polarity, such as is presented by the AT sequences.[31] Actually, we were surprised by the lack of fluorescence quenching upon intercalation of MPIM into this polynucleotide. In fact, fluorescence suppression of pyrene when intercalated into AT-rich regions is quite common. This process is due to a proton-assisted photooxidative pathway consisting of a photoinduced electron transfer from the singlet state of pyrene to the T residues followed by a rapid proton transfer from water to the $T^{\bullet -}$ electron adduct.[32–34] It is well-known that such a protonation step is crucial for the photoinduced electron transfer to occur, since it lowers the free energy by about 0.9 eV.[34] At this point the origin of the observed behavior appears unclear. A tentative explanation could be that the non-planar isoxazolidine substituent hinders, to some extent, the above protonation pathway. Such an effect could increase the value of the free energy making it insufficient to drive the overall photoinduced electron transfer process. The quenching experiments with iodide would seem to be in line with this picture. In fact, the K_{SV} value measured in the absence of polynucleotides drops *ca.* 30-fold in the presence of poly-d(AT)$_2$. Such a difference in the K_{SV} values between water and poly-d(AT)$_2$ is larger than that typically observed for other intercalative pyrene derivatives characterized by higher binding constants with the same polynucleotide.[10] This suggests that, whatever the exact localization of MPIM, an additional shielding contribution to the polar quencher could derive from the isoxazolidine ring.

The preference for intercalation of MPIM into the AT sites would not seem surprising if one considers that these sequences offer a less polar environment than GC sites, to the non-polar pyrenyl chromophore.[31] However, it should be taken into account that polycyclic intercalators such as pyrene and anthracene derivatives bearing only small substituents, do not exhibit any preferential binding for either AT or GC sequences.[5,6] On these grounds, it emerges that the isoxazolidine *N*-substituent may play a role in inducing a certain degree of selectivity for the AT sites, as observed from calculations. This hypothesis is in good agreement with literature data regarding pyrene derivatives bearing piperazinyl substituents

for which some selectivity for base pairs intercalation has been observed.[35]

As far as the binding of MPIM to poly-d(GC)$_2$ is concerned, the quenching results in the presence of iodide uphold what was proposed on the basis of the absorption data. The K_{SV} value found in this case only slightly differs from that measured in the absence of polynucleotide, pointing to a higher accessibility of the quencher to the fluorophore in accordance with a shallow intercalation of MPIM into these alternate sequences. This lower level of intercalation is not in contrast with the effective fluorescence quenching observed (see Fig. 5). Since the singlet state energies of the DNA bases[36] are at least 1.2 eV greater than that of MPIM, the quenching through an energy transfer mechanism is, of course, out of question. Rather, the fluorescence suppression can be attributable to a photoreductive pathway involving an energetically favoured photoinduced electron transfer from the guanine residues to the excited chromophore. Indeed, by assuming that the reduction potential of the pyrene unit of MPIM is similar to that of pyrene, $E^{\circ}(\text{MPIM}/\text{MPIM}^{\bullet -}) = -1.85$ V *vs.* NHE (normal hydrogen electrode), the reduction potential of the guanine residues in neutral aqueous solution is $E^{\circ}(G^{\bullet +}(-H^{+})/G) = 1.29$ V *vs.* NHE, that the energy of the excited singlet state of MPIM $\Delta E_{0,0} = 3.28$ eV, and that the coulombic energetic term, w, characterizing the interaction between the two radical pairs is <0.1 in water solution,[37] it can be readily noted that the thermodynamic balance based on the Rehm–Weller eqn (6) [38] is negative, making the photoreductive pathway highly feasible.

$$\Delta G^{\circ} = \text{e}[E^{\circ}(G^{\bullet +}(-H^{+})/G) - E^{\circ}(\text{MPIM}/\text{MPIM}^{\bullet -})] - \Delta E_{0,0} + w \quad (6)$$

This type of quenching mechanism is very common even for pyrene units not deeply intercalated but only nearby to GC sites,[10,32,37]

The results obtained in the presence of ct-DNA reflect fairly well the preference of the pyrene derivative for the AT sequences and also agree with the values of both experimental and calculated binding constants. In particular, it can be noted that the absorption spectrum obtained at the highest concentration of DNA [see Fig. 2(A)], corresponding to the almost totally bound form of MPIM, closely resembles that obtained in the presence of poly-d(AT)$_2$ under similar experimental conditions [see Fig. 2(B) for comparison]. Besides, the emission features are also similar to those with poly-d(AT)$_2$ (compare inset Fig. 3 with Fig. 4). The slight fluorescence quenching noted might be attributable to the small fraction of molecules of MPIM close to the GC sites where, as described above, effective photoinduced electron transfer may occur. Finally, the K_{SV} constant obtained indicates a good degree of protection from the ionic quencher in accordance with the preferential localization of MPIM in AT-rich regions.

Conclusions

MPIM binds to double-stranded polynucleotides with binding constants in the range 1–7 $\times$ 10^3 M^{-1}, in DNA base pairs, indicating a good affinity for the double helix. The strong hypochromism, the fluorescence data and the Stern–Volmer constants observed in the presence of an anionic quencher such as iodide, strongly support an intercalative binding mode of the chromophore in the case of ct-DNA and poly-d(AT)$_2$ whereas a shallow intercalation seems to be involved with poly-d(GC)$_2$. These results are well corroborated by docking studies which also evidence (i) that intercalation is taking place from the major groove of the double helix and (ii) a contribution derived from a hydrogen bond to the stability of the resulting complex.

It appears clear that the presence of the isoxazolidine substituent in the structure of MPIM, besides conferring satisfactory solubility in aqueous medium, seems also to play a role in determining some preference for alternating AT rather than for GC sequences. This is probably due to a more snug fit of MPIM into the major groove of the d(AT) due to the steric hindrance observed between the isoxazolidinic *N*-methyl and the amino group of cytosine.

The study presented herein well complements our recent investigation, pointing out that the biological properties of MPIM may be related to its direct interaction with DNA. In this respect, in view of the differential dependence of the fluorescence properties of MPIM on the DNA sequences, further investigations addressed to explore the DNA-cleavage induced by MPIM upon light excitation, may represent a worthwhile objective to pursue. Such photoinduced activity could in fact be exploited in combination with the thermal biological properties displayed by MPIM in order to produce synergistic effects.

Acknowledgements

We thank the MIUR (PRIN research projects, Rome, Italy) for the financial support.

References

1 (*a*) U. Pindur, M. Haber and K. Sattler, *J. Chem. Educ.*, 1993, **70**, 263; (*b*) S. P. Gupta, *Chem. Rev.*, 1994, **94**, 1507; (*c*) S. Sortino and G. Condorelli, *New J. Chem.*, 2002, **26**, 250; (*d*) S. Sortino, S. Giuffrida and J. C. Scaiano, *Chem. Res. Toxicol.*, 1999, **12**, 971.
2 D. W. Henry, *Cancer Treat. Rep.*, 1979, **63**, 845.
3 W. A. Denny, B. F. Cain, G. J. Atwell, C. Hansch, A. Panthananickal and A. Leo, *J. Med. Chem.*, 1982, **25**, 276.
4 L. F. Liu, *Annu. Rev. Biochem.*, 1989, **58**, 351.
5 See, for example: (*a*) C. V. Kumar, A. L. Raphael and J. K. Barton, *J. Biomol. Struct. Dyn.*, 1986, **3**, 85; (*b*) N. E. Geacintov, T. Prusik and J. M. Khosrofian, *J. Am. Chem. Soc.*, 1976, **98**, 6444; (*c*) H. C. Becker and B. Nordèn, *J. Am. Chem. Soc.*, 1999, **121**, 11947; (*d*) C. V. Kumar and E. H. Asuncion, *Chem. Commun.*, 1999, 1219.
6 C. V. Kumar, R. S. Turner and E. H. Asuncion, *J. Photochem. Photobiol., A*, 1993, **74**, 231.
7 N. E. Geacintov, D. Zinger, V. Ibanez, R. Santella, D. Grumberger and R. G. Harvey, *Carcinogenesis*, 1987, **8**, 925.
8 C. V. Kumar, E. H. A. Punzalan and W. B. Tan, *Tetrahedron*, 2000, **56**, 7027.
9 C. V. Kumar and E. H. Asuncion, *J. Am. Chem. Soc.*, 1993, **115**, 8547.
10 M. E. C. D. Real Oliveira, A. L. Baptista, P. J. G. Coutinhoo, E. M. S. Castanheira and G. Hungerford, *Photochem. Photobiol. Sci.*, 2004, **3**, 217.
11 A. Rescifina, M. A. Chiacchio, A. Corsaro, E. De Clercq, D. Iannazzo, A. Mastino, A. Piperno, G. Romeo, R. Romeo and V. Valveri, *J. Med. Chem.*, 2006, **49**, 709.
12 (*a*) U. Chiacchio, D. Iannazzo, A. Rescifina and G. Romeo, *J. Org. Chem.*, 1999, **64**, 28; (*b*) U. Chiacchio, A. Corsaro, G. Gumina,

A. Rescifina, D. Iannazzo, A. Piperno, G. Romeo and R. Romeo, *J. Org. Chem*., 1999, **64**, 9321; (*c*) U. Chiacchio, A. Corsaro, D. Iannazzo, A. Piperno, V. Pistarà, A. Rescifina, R. Romeo, V. Valveri, A. Mastino and G. Romeo, *J. Med. Chem*., 2003, **46**, 3696; (*d*) U. Chiacchio, E. Ballistreri, B. Macchi, D. Iannazzo, A. Piperno, A. Rescifina, R. Romeo, M. Saglimbeni, M. T. Sciortino, V. Valveri, A. Mastino and G. Romeo, *J. Med. Chem*., 2005, **48**, 1389.
13 J. K. Barton, J. M. Goldberg, C. V. Kumar and N. J. Turro, *J. Am. Chem. Soc*., 1986, **108**, 2081.
14 W. D. Cornell, P. Cieplak, C. I. Bayly, I. R. Gould, K. M. Merz, D.M. Ferguson, D. C. Spellmeyer, T. Fox, J. W. Caldwell and P. A. Kollman, *J. Am. Chem. Soc*., 2005, **117**, 5179.
15 Hyperchem, Release 7.5, Hypercube Inc., Gainesville, FL, USA.
16 (*a*) K. V. Miroshnychenko and A. V. Shestopalova, *Mol. Simul*., 2005, **31**, 567; (*b*) A. S. F. Osvaldo and F. V. Daniel, *Bioorg. Med. Chem. Lett*., 1997, **7**, 1797.
17 E. Katchalski-Katzir, I. Shariv, M. Eisenstein, A. A. Friesem, C. Aflalo and I. A. Vasker, *Proc. Natl. Acad. Sci. U. S. A*., 1992, **89**, 2195. Gramm version 1.03 is distributed for free: http://www.bioinformatics.ku.edu/research/vakser/resources/gramm/gramm1.
18 D. C. Dong and M. A. Winnik, *Can. J. Chem*., 1984, **62**, 2560.
19 S. Hashimoto, *J. Phys. Chem*., 1993, **97**, 3662.
20 A. M. Pyle, J. P. Rehmann, R. Meshoyer, C. V. Kumar, N. J. Turro and J. K. Barton, *J. Am. Chem. Soc*., 1989, **111**, 3051.
21 N. E. Geacintov, *Photochem. Photobiol*., 1987, **45**, 547.
22 J. R. Lakowicz, *Principles of Fluorescence Spectroscopy*, Plenum Press, New York, 1983.
23 C. V. Kumar and E. H. Asuncion, *J. Chem. Soc., Chem. Commun*., 1992, 470.
24 H. P. Nelson and H. DeVoe, *Biopolymers*, 1984, **23**, 897.
25 N. E. Geacintov, M. Shahbaz, V. Ibanez, K. Moussaoui and R. G. Harvey, *Biochemistry*, 1988, **27**, 8380.
26 H. Suenaga, K. Nakashima, T. Mizuno, M. Takeuchi, I. Hamachi and S. Shinkai, *J. Chem. Soc., Perkin Trans. 1*, 1988, 1263.
27 C. V. Kumar, in *Photochemistry in Organized and Constrained Media*, ed. V. Ramamurthy, VCH Publisher, New York, 1991, pp. 785–816.
28 E. C. Long and J. K. Barton, *Acc. Chem. Res*., 1990, **23**, 271.
29 K. Kalyanasundaram and J. K. Thomas, *J. Am. Chem. Soc*., 1977, **99**, 2039.
30 D. C. Dong and M. A. Winnik, *Photochem. Photobiol*., 1982, **35**, 17.
31 W. Muller and D. M. Chrothers, *Eur. J. Biochem*., 1975, **54**, 267.
32 V. Y. Shafirocich, S. H. Courtney, N. Ya and N. E. Geacintov, *J. Am. Chem. Soc*., 1995, **117**, 4920.
33 M. Manooharan, K. L. Tivel, M. Zhao, K. Nafisi and T. L. Netzel, *J. Phys. Chem*., 1995, **99**, 17461.
34 S. Steenken, J. P. Telo, H. M. Novais and L. P. Candeias, *J. Am. Chem. Soc*., 1992, **114**, 4701.
35 H. C. Becker and B. Nordèn, *J. Am. Chem. Soc*., 2000, **122**, 8344.
36 J. Cadet and P. Vigny, in *Bioorganic Photochemistry*, ed. H. Morrison, Wiley Interscience, New York, 1990, pp. 1–272.
37 N. E. Geacintov, V. Y. Shafiroovich, B. Li, B. Mao and N. Ya, *Spectrum (Bowling Green, OH, U. S.)*, 1997, **10**, 1.
38 D. Rehm and A. Weller, *Isr. J. Chem*., 1970, **8**, 259.